Effect of the microstructure parameters on the Mullins softening in carbon-black filled SBRs

Yannick Merckel[1], Julie Diani[21], Mathias Brieu[1], Pierre Gilormini[2], Julien Caillard[3]

[1]LML, Ecole Centrale de Lille, bd Paul Langevin, 59650 Villeneuve d'Ascq, France

[2]Laboratoire PIMM, CNRS, Arts et Métiers ParisTech, 151 bd de l'Hôpital, 75013 Paris, France

[3]Manufacture Française des Pneumatiques Michelin, CERL, Ladoux, 63040 Clermont-Ferrand, France

ABSTRACT:

A quantitative estimate of the Mullins softening is proposed and tested on various carbon-black filled styrene-butadiene rubbers. In order to model the behaviour of elastomeric materials, some constitutive equations reported in the literature are based on the account of a strain amplification factor, which evolves with the maximum strain history. The amplification factor is grounded on the representation of filled rubbers as heterogeneous materials made of hard rigid domains and soft deformable domains. In the present work, this factor is splitted into two parts with opposite effects that account for the Mullins softening and for the filler reinforcement, respectively. Evolutions of both parts are obtained through a direct analysis of cyclic uniaxial tensile tests performed on a series of materials. The Mullins softening part is shown to linearly depend on the filler volume fraction and on the maximum strain applied, when defined as the first invariant of the Hencky tensor. Its changes with the gum crosslink density parameter are insignificant. The reinforcement part of the amplification factor shows quadratic dependence on the filler volume fraction.

Key words:

Rubber, Fillers, Reinforcement, Mullins softening, Strain amplification factor

[1] Corresponding author: julie.diani@ensam.eu

INTRODUCTION

Adding fillers in a non-crystallizing rubber changes its mechanical behaviour in many ways [1]. Fillers increase the material stiffness, introduce a substantial stress-softening at the first load known as the Mullins effect, and modify the material viscosity. The fillers are understood to act as reinforcements at a continuum scale, which explains the stiffening effect[2]. At a molecular level, their influence is still debated, but it is clear that they introduce a local evolution of the microstructure when the material is first stretched, which results in the development of the Mullins effect [3,4].

Mullins and Tobin[5] introduced the concept of strain amplification in filled rubbers in order to account for the reinforcement at large strains of an elastomer when filler particles and particle clusters are included into the gum. The filled rubber is described as co-existing hard and soft domains. The rigid hard domains are assumed to remain undeformed, therefore the soft ones undergo a larger strain than the average strain applied to the material. The strain in the soft regions is then the applied strain amplified by a factor which is increasing with the increase of filler volume fraction. This strain amplification notion was extended to various strain measures[5,6,7,8] to account for the filler reinforcement within the context of hyperelasticity.

Later, the strain amplification factor was extended to the case of hyperelasticity with Mullins softening, using an early idea suggested by Mullins and Tobin[9], where the amount of hard phase depends on strain history. The Mullins effect is then understood as an irreversible breakdown of filler-clusters [10] which results in a decrease of the volume fraction of hard domains. This physical interpretation of the Mullins stress-softening was used in a number of contributions [11-16], where an amplification factor decreasing with the maximum applied strain is defined.

In this study, we will apply and revise the amplification factor concept in order to quantify the effect of the microstructure parameters on the Mullins softening. We will compare the stress-strain responses of different non-crystallizing filled styrene-butadiene rubbers submitted to various strain levels, and thus undergoing a substantial Mullins effect. Materials will be characterized by their crosslink density and their amount and type of fillers. The objective will be to identify the evolution of the strain amplification factor as a function of the material parameters and the applied loading history. In contrast with previous studies [7,12-16], we will not assume any mathematical form for the strain amplification factor for that the experimental data analysis will reveal it. We will consider a large number of materials, composed of SBR

gum with crosslink densities varying from 3 to 11 (10^{-5} mol/cm^3) and filled with an amount of carbon-black from 5 to 60 parts per hundred rubber (phr). Finally, three types of carbon-black are considered in order to also highlight the size effect of particles.

The next section reviews the basic equations required for the experimental data analysis. Then, the material strategy and the tests run for the characterization of the mechanical behaviour of the materials are reported. In following sections, results are presented and discussed. Concluding remarks close the paper.

BASIC EQUATIONS

Using Mullins and Tobin[5] representation, a filled rubber is described by an heterogeous material made of hard rigid domains and soft deformable domains. The hard domains consist of filler particles and particle aggregates which contain a fraction of the gum (trapped rubber between fillers aggregates that have formed agglomerates[2]). The hard domains are rigid and therefore the soft domains undergo a larger strain than the strain applied to the filled rubber. The strain in the soft region is actually amplified by a strain amplification factor. The stresses are assumed homogeneous within the material and therefore the stresses are identical in the hard domains and in the soft domains.

Initially, when the filled rubber is still virgin of any load, the strain sustained by the soft regions, Λ^{soft}, is assumed to be amplified of a factor $X>1$:

$$\Lambda^{soft} = X\,\Lambda^{virgin} \tag{1}$$

Λ^{virgin} being the strain that would undergo the virgin rubber. The parameter X characterizes the initial strain amplification factor and depends on the material microstructure. But the behaviour of a filled rubber evolves when first stretched; actually, it is well known that the initial rubber softens due to the Mullins effect. This can be explained by a breakdown of filler particles and particle clusters reducing the amount of hard domains in the material. In the strain amplification framework, this can be taken into account by introducing a reduction $(1-D)$ of the parameter X,

$$\Lambda^{soft} = X\,(1-D)\,\Lambda \tag{2}$$

where Λ is the strain undergone by the actual filled rubber during the mechanical test. The parameter D may be considered as a damage parameter representing the Mullins softening and depending on the loading history. Hence, D evolves according to the maximum strain applied and $D=0$ when the material has never been stretched.

At this point, let us note that equation (2) is a generalization of previous works. For example, the concept of Mullins and Tobin[5] comes by setting, $\Lambda=\lambda-1$, with λ denoting the stretch, and by assuming that D is zero. Otherwise, by setting $\Lambda=I_1-3$ where I_1 is the first invariant of the left Cauchy Green tensor $\boldsymbol{C}=\boldsymbol{F}^t.\boldsymbol{F}$ (where $\boldsymbol{F}$ denotes the deformation gradient), and still assuming that D is zero, the relation proposed by Bergstrom and Boyce[7] is obtained. Let us note that in both cases, the Mullins softening is not taken into account and the strain amplification factor X is a quadratic function of the volume fraction of fillers. A general form is $X=1+a\ \varphi\ +b\ \varphi^2$, φ being the volume fraction of filler and, a and b depending on the fillers morphology and on the definition of Λ.

When the Mullins softening is taken into account, our variables D and X are usually grouped into a single variable equal to $X(1-D)$. For example, by setting $\Lambda=\lambda-1$ and by assuming that the product $X(1-D)$ is a function of φ and a power or exponential law of λ_{max}, eq. (2) becomes equivalent to the relations proposed by Kluppel and Schramm[12]. The latter model is extended to general three-dimensional deformation states by Luo et al.[14] where $\Lambda=\lambda_i-1$ and the product $X(1-D)$ follows a power law governed by the maximum of I_1. This three-dimensional approach is also used by[15,16].

An interest of the present study is to deduce the evolutions of X and D from experimental analysis without postulating any mathematical forms a priori. These evolutions are strongly dependent of the definition of Λ, which must be chosen carefully. In order to extend to general three-dimensional deformation states, the second invariant of the Hencky strain tensor $\boldsymbol{h}=(1/2)\ \ln\ (\boldsymbol{F}^t.\boldsymbol{F})$ is adopted for the strain measure,

$$\Lambda = H = \sqrt{\frac{2}{3}(h_1^2 + h_2^2 + h_3^2)} \tag{3}$$

where $h_i=ln(\lambda_i)$, with λ_i being the principal stretches. This original choice was also motivated by the results from[12] showing an exponential law or a power law evolution for the strain amplification factor.

Parameters X and D are estimated from data provided by cyclic uniaxial tension tests. The material strategy and the experimental tests are detailed in the next section.

MATERIAL EXPERIMENTS

Materials

For this study, Michelin prepared various carbon-black filled styrene-butadiene rubbers (SBR). The material strategy was to vary a single parameter at a time in order to clearly identify the key factors involved in the mechanical behaviour and Mullins softening of filled rubbers. The components of the reference material M1 are listed in Table I. Materials M2, M3, M4 and M5 are obtained from material M1 by changing the amount of carbon-black to 5, 30, 50 and 60 phr, respectively. Materials M6 and M7 are equivalent to material M1 except for the type of carbon-black. The compositions of materials M11, M16, M17, listed in Table II, result in materials with the same amount and the same type of carbon-black fillers than M1 but with various crosslink densities. Finally, materials M12, M13, M14 and M15 are similar to M11 except for the amount of carbon-blacks. Fig. 1 sketches the material strategy.

The actual crosslink densities of all these materials were measured by swelling and the results are given in Table III. The uncertainty of the measure is 0.3×10^{-5} mol/cm^3. Carbon-black fillers used in M1, M6 and M7 are N347, N326 and N550, respectively. They are of the same nature but with various morphologies that depend on the fineness of the elementary particle and on the aggregate structure. The fineness corresponds to a specific surface area of fillers, it is measured by nitrogen gas absorption (N_2S absorption) using the Brunner Emmet Teller analysis (BET). The aggregate structure, which characterizes the branching of the aggregates, is measured by dibutyl-phthalate absorption (DBP absorption). The results of the morphology analysis are listed in Table II and the values of the filler volume fraction φ are reported in Table III for all materials. Every material was tested in uniaxial tension according to the same test described below.

Mechanical testing

Mechanical tests were conducted on an Instron 5882 uniaxial testing machine with a 2 kN load cell. Flat dumbbell specimens of normalized geometry, 30 mm long, 4 mm wide and 2.5 mm thick, were considered. Tests were run in displacement control at an extension rate of 0.3 mm/s. Local strain was measured by video extensometry. Samples were submitted to cyclic uniaxial tension until break. At each cycle the maximum strain increased with a step of

$ln(l/l_0)=0.1$, the minimum of the cycles was set to a null force in order to avoid any specimen buckling.

As expected for filled rubbers, the materials show a substantial softening when first loaded to an amount of strain never undergone before. Fig. 2 illustrates the cyclic stress-strain response of material M1 in terms of Cauchy stress σ with respect to the Hencky strain measure H. This softening is known as the Mullins effect (see[3,4] for reviews on the matter) and increases with the applied macroscopic strain. Once the Mullins effect is released, one may notice that at low strain rate, the unloading and the reloading stress-strain responses are fairly close (Fig. 2) and the material behaviour after Mullins softening may be characterized on both the unloading and the reloading paths. Fig. 3 shows that the potential viscous component of the stress is larger during the loading than the unloading. Therefore, in what follows, the unloading stress-strain responses of a material will be used to characterize its Mullins softened hyperelastic stress-strain responses. Considering the second loading stress-strain responses instead, one would observe small changes in the values presented here but the main core of our results would remain.

Along with the material softening, one notes a permanent set, λ_{perm}, increasing with the applied maximum strain H_{max}. Part of this set can be recovered with time but a substantial part remains. Modeling the permanent set would require introducing some anisotropy[17]. This would add an unnecessary complexity to our arguments without benefiting the results presented here. Considering the unloading responses obtained during a single cyclic test is conveniently fast but is not representative of the stress-strain responses that would be measured by a user unaware of the loading history. Therefore in order to reach the material stress-strain response that would measure such a user, and which is the actual stress-strain response of the softened material, we need to correct the measured stretch λ^{meas} by the permanent set according to the relation:

$$\lambda = \lambda^{meas} / \lambda_{perm} \tag{4}$$

Doing so, the responses of material M1 corresponding to various level of softening are presented Fig. 4. Such a permanent set filter procedure is common when dealing with Mullins softening and permanent set. In the following, all our data were modified according to eq. (4).

As expected, our materials showed a Mullins softening effect that varies from one material to another, exhibiting a microstructural dependence of the effect. It is already known from a qualitative standpoint that the Mullins softening increases with an increase of the amount of

fillers in SBR gums[12,14,18] as in other types of gums[7,9,19-21]. In the next section, such representations of the Mullins effect as shown in Fig. 4 will be used to extract *X* and *D*, and to study their evolutions with the material parameters and the applied level of strain.

MICROSTRUCTURE AND LOADING INTENSITY DEPENDENCE OF THE MULLINS SOFTENING *D*

In this section, we will focus on the evolution of the softening parameter *D* with the maximum loading reached and with the microstructure parameters φ and N_c. First, the method used to obtain the evolution of *D* with the loading intensity is presented. Then, the evolutions of *D* from one material to another are analyzed, in order to evaluate the roles of the material parameters.

Method

As explained in the basic equations section, the softening parameter *D* defines the relationship between the behaviour of a virtual material, virgin of any load, and the actual behaviour of the filled elastomer, which is measured experimentally.

For each material, parameter *D* varies with the maximum strain H_{max} only, and is therefore constant along each unloading path. Using the experimental stress-strain responses as presented in Fig. 4 for material M1, it is possible to calculate a value of *D* for each unloading response in such a way that all curves superimpose onto a master curve. When using the condition $D=0$ for $H_{max}=0$, the obtained master curve represents the mechanical behaviour of the virtual virgin material. Let us remind that the latter behaviour is dependent of the type of microstructure, the nature of the gum, the amount and type of fillers.

Values of *D* are computed using a least squares minimization. Fig. 5 shows the results obtained from the softened stress-strain responses of material M1 shown in Fig. 4. A good superposition of the curves is observed in Fig. 5, which supports the concept of a master curve representing the mechanical behaviour of a material virgin of loading. The inset figure in Fig. 5 presents the computed values of the parameter *D* vs. the maximum strain: it increases with the maximum strain, which means that softening is enhanced by loading intensity, and this increase is quasi-linear, which corroborates former results from[12] showing an exponential evolution of *D* with maximum stretch, and this also justifies the choice of *H* as the strain measure. We used this procedure for each material in order to access to the evolution of *D* with H_{max} for all materials. In the next section we present the results that have been obtained.

Results

We are interested in the comparison of the evolutions of $D(H_{max})$ for various materials in order to identify the effects on D of the crosslink density, the filler volume fraction and the type of fillers. First, we compare the evolutions of D for materials M1, M11, M16 and M17. These materials are filled with an amount of 40 phr of fillers N347, which corresponds approximately to a 16.6% volume fraction, and show crosslink densities ranging from 3.65 to 10.55 10^{-5} mol/cm^3. The latter value is very close to the maximum crosslink density that can be reached with the material mixes considered here. Fig. 6 shows the values of $D(H_{max})$ for these materials. Two important features can be observed in this figure: the maximum strain at break decreases when N_c increases, and the evolution of D is similar for the four materials considered.

Next, we confront the evolutions of D for materials M1, M2, M3, M4 and M5 in order to investigate the effect of the amount of fillers on the Mullins softening. Actually material M2 shows little Mullins effect, for it contains only 5 phr of fillers (see Fig. 10). Materials M1, M3, M4 and M5 contain 40, 30, 50 and 60 phr, respectively, and have similar crosslink densities ($N_c \sim 7.10^{-5}$ mol/cm^3). Fig. 7 shows the evolutions of D for these materials. One notices immediately the strong impact of the filler amount on the slope of the D curve, which attests for a major effect on the Mullins softening. This softening increases with the increase of filler fraction. The evolutions of D corresponding to materials M11, M13, M14, M15 were also computed and are similar to the evolutions presented here for M1, M3, M4 and M5 respectively, confirming the minor effect of the crosslink density parameter on D.

Finally, in order to study the effect of the type of fillers, Fig. 8 shows the evolution of D for materials M1, M6 and M7 with similar crosslink densities and amounts of carbon-black fillers, but with various types of fillers: N347, N326 and N550, respectively (see Table II for the characteristics of the fillers). Fig. 8 shows a minor effect of the type of filler compared to the effect of the amount of filler, although this effect seems larger than the effect of the crosslink density N_c. Here, we limited our study to a small number of types of carbon-black fillers. The results could have been different if the study included other types of filler than carbon-black. For instance, Luo et al.[14] compared the softening in SBRs filled by carbon-black N220 or by silica-silane, and showed that the nature of the filler has a substantial impact on the material softening, with carbon-black fillers showing a stronger adsorption or binding

ability. Subsequent experimental work would be necessary to provide a final and complete opinion on this aspect.

Analysis

The interest of parameter D as it is defined here stands in its ability to provide a direct comparison of the softening of materials characterized by very different microstructure parameters (nature of the gum, nature, type and amount of fillers), and therefore by different mechanical properties (stiffness, stretch at failure, etc.). For the materials of the present study, the analysis of the experimental data (Fig. 6-8) shows a linear dependence of D on H_{max}, which writes:

$$D = \alpha H_{max} \quad (5)$$

Fig. 6 assesses that parameter α does not depend on the crosslink density parameter N_c and Fig. 7 shows its strong dependence on φ. Hitherto, the Mullins softening was interpreted either by chain desorption at the filler interface and breakdown of agglomerates[22,23] or by a change in the rubber phase only[19]. The fact that the Mullins softening is not affected by a change in the gum crosslink density, and therefore in the gum properties, for the same amount of filler, favors the physical interpretation in terms of the desorption and particle cluster breakdown.

In order to quantify how D changes with the filler volume fraction, values of α are plotted vs. φ in Fig. 9. One notes a good agreement between the experimental data and the linear approximation:

$$\alpha(\varphi) = 2.623\ (\varphi - 0.068\ ) \quad (6)$$

This approximation suggests that there exists a threshold of filler content φ_0=0.068, below which the Mullins softening can be neglected. We have not been able to access to materials containing this amount of fillers exactly, but we have checked that materials containing 5 phr, or equivalently a volume fraction of 0.02, do not show any significant Mullins effect (Fig. 10).

Finally, the analysis of the experimental data reveals a remarkably simple form for D, which writes:

$$D(\varphi, H_{max}) = \beta\ (\varphi - \varphi_0)\ H_{max} \quad (7)$$

with β and φ_0 being two parameters that supposedly depend on the binding ability of the filler with the gum. The latter property is also evidenced in the factor X which is analyzed below.

MICROSTRUCTURE DEPENDENCE OF STRAIN AMPLIFICATION FACTOR *X*

In the previous section, we studied how the filler reinforcement is evolving in filled rubbers according to the maximum stretching applied. This provided us with the evolution of the damaging parameter *D*. This process involved a master curve, which defined the stress-strain behaviour of the virgin material and was obtained for *D=0,* for each actual material. In the present section, we are interested in how the behaviour of the virgin material relates to the behaviour of the soft domains, which is disclosed by the reinforcement parameter *X*.

Method

The strain amplification factor *X* accounts for the initial reinforcing effects of fillers and filler aggregates embedded in the soft matrix. As defined by eq. (1), this factor relates the mechanical behaviour of a filled rubber without softening to the mechanical behaviour of the soft domains. It allows comparing the behaviour of materials with a similar gum matrix and various amounts of fillers, corresponding to various fractions of hard domains, to the behaviour of the soft domains. Processing and testing pure SBR gums is not an easy task, with cavities appearing easily during the manufacturing process. For this reason, a low amount of 5 phr ($\varphi \sim 0.02$) of carbon-black was added to gums characterized by crosslink densities of 7.10^{-5} mol/cm^3 and $10.55.10^{-5}$ mol/cm^3, providing materials M2 and M12. These materials present a very limited Mullins effect as shown in Fig. 10, and their low but non null filler content makes them likely to exhibit a mechanical behaviour close to the mechanical behaviour of the soft domains with minimum amounts of hard domains. Reading the material strategy shown in Fig. 1, one distinguishes two sets of materials M1, M2, M3, M4, M5, and M11, M12, M13, M14, M15 where crosslink density does not vary in each set. Fig. 11 shows the master curves for the stress-strain responses of virgin materials M1 to M5 and M11 to M15, which have similar crosslink densities of 7.10^{-5} mol/cm^{3}and 10.10^{-5} mol/cm^3, respectively. As expected, adding carbon-black stiffens the materials.

For both sets of materials characterized by the same crosslink densities, values of the intensity factor *X* are computed according to (1) so as to get the best superimposition of the stress-strain responses of virgin materials containing various amounts of fillers. This procedure is identical to the procedure used in the previous Method section but instead of comparing the stress-strain responses of the same material submitted to various levels of maximum strain, one compares the stress-strain responses for *D=0* for materials made with the same crosslink density and with different filler fractions. Fig. 12 shows the superimpositions of the

mechanical behaviours of materials M1 to M5 and M11 to M15. Results are fairly good and supply values of the strain amplification factor X for five filler fractions for both gums. These values are plotted and analyzed in the next section.

Results and analysis

Fig. 13 displays the values of X obtained when producing Fig. 12 for various filler volume fractions φ. These values appear to be independent of N_c, but this result is balanced by the high sensitivity of X to the superposition procedure. Actually, it would be necessary to extend the procedure to other values of N_c to decide about the range of validity of this result. It may also be noted that X shows a quadratic dependence on φ. This supports former quadratic results from the literature[7,13] inspired by the Guth-Gold[24] quadratic infinitesimal strain model. It is remarkable to read in Fig. 13 that a quadratic function defined as:

$$X(\varphi) = 1 + a\,\varphi + b\,\varphi^2 \qquad (8)$$

provides a good fit of the X values.

CONCLUSION

In this contribution, we revisited the strain amplification factor theory in order to propose a quantitative estimate of the Mullins effect that provides a direct comparison of various materials. Several carbon-black filled styrene-butadiene rubbers, with various crosslink densities, amounts of fillers and types of fillers, were tested in cyclic uniaxial tension. The decomposition of the strain amplification factor into a softening part D and a reinforcing part X, coupled with an original analysis of the experimental data, gave access to a quantitative estimate of the Mullins softening for each material. This softening exhibited a negligible dependence on the crosslink density, a weak influence of the filler type, and a linear increase with the filler volume fraction. It also appears to be linearly dependent on the maximum strain when the latter is written as the first invariant of the Hencky strain tensor.

The reinforcing character of the fillers was also evaluated for two SBR gums characterized by different crosslink densities through the definition of suitable virgin virtual materials, which are assumed to behave like equivalent filled rubbers without Mullins effect. Comparison between the various materials showed that the reinforcing factor X depends quadratically on the filler volume fraction, which corroborates former results of the literature.

Acknowledgments

This work was supported by the French "Agence Nationale de la Recherche" through project AMUFISE (MATETPRO08-320101). The authors acknowledge useful discussions with D. Berghezan, C. Creton, J. de Crevoisier, F. Hild, C. Moriceau, M. Portigliatti, S. Roux, F. Vion-Loisel, and H. Zhang.

References

1. Bergström, J. S. Ph.D. thesis, Massachusetts institute of technology, 1999.
2. Kohls, D.; Beaucage, G. Curr. Opin .Solid State Mat. Sci. 2002, 6, 183.
3. Mullins, L. Rubber Chem. Technol. 1969, 42, 339.
4. Diani, J.; Fayolle, B.; Gilormini, P. Eur. Polym. J. 2009, 45, 601.
5. Mullins, L.; Tobin, N. R. J. Appl. Polym. Sci. 1965, 9, 2993.
6. Govindjee, S.; Simo, J. C. J. Mech. Phys. Solids 1991, 39, 87.
7. Bergström, J. S.; Boyce, M. C. Rubber Chem. Technol 1999, 72, 633.
8. Dargazany, R.; Itskov, M. Int. J. Solids and Struct. 2009, 46, 2967.
9. Mullins, L.; Tobin, N. R. Rubber Chem. Technol. 1957, 30, 555.
10. Krauss, G.; Childers, C.; Rollman, K. J. Appl. Polym. Sci. 1966, 10, 229.
11. Johnson, N. A.; Beatty, M. F. Contin. Mech. and Thermodyn. 1993, 5, 83.
12. Klüppel, M.; Schramm, J. Macromol. Theory. Simul. 2000, 9, 742.
13. Qi, H.; Boyce, M. J. Mech. Phys. Solids 2004, 52, 2187.
14. Luo, H.; Klüppel, M.; Schneider, H. Macromolecules 2004, 37,8000.
15. Meissner, B.; Matějka, L. Polymer 2006, 47, 7997.
16. Meissner, B.; Matějka, L. Eur. Polym. J. 2008, 44, 1940.
17. Diani, J.; Brieu, M.; Vacherand, J. Eur. J. Mech. Solids A 2006, 25, 483.
18. Kar, K. K.; Bhowmick, A. K. Polym. Eng. Sci. 1998, 38, 1927.
19. Harwood, J. A. C.; Mullins, L.; Payne, A. R. Appl. Polym. Sci. 1965, 9, 3011.
20. Dorfmann, A.; Ogden, R. W. Int. J. Solids and Struct. 2004, 41, 1855.
21. Harwood, J. A. C.; Payne, A. R. J. Appl. Polym. Sci. 1966, 10, 315.
22. Blanchard, A. F.; Parkinson, D. Ind. Eng. Chem. 1952, 44, 799.
23. Blanchard, A. F.; Parkinson, D. J. Appl. Polym. Sci. 1960, 5, 107.
24. Guth, E.; Gold, O. Phys. Rev. 1938, 53, 322.

TABLE I

Material composition in parts per hundred rubber (phr)

Ingredient	M1	M11	M16	M17
SBR	100	100	100	100
Carbon-black (N347)	40	40	40	40
Antioxidant (6PPD)	1.9	1.9	1.9	1.0
Stearic acid	2.0	2.0	2.0	0
Zinc oxide	2.5	2.5	2.5	0
Structol ZEH	0	0	0	3
Accelerator (CBS)	1.6	2.3	1.0	1.5
Sulfur	1.6	2.3	1.0	1.5

Table II

Carbon-black morphology and characterization

Filler morphology	Characterization	N347	N326	N550
Structure	DBP (ml/100g)	120	70	125
Fineness	BET (m2/g)	90	79	41

Table III

Microstructure parameters, cross-link density *Nc* and filler volume fraction Φ

Material	*Nc* (10^{-5} mol/cm^3)	Φ (%)
M1	7.38	16.65
M2	6.53	2.43
M3	8.16	13.03
M4	8.26	19.98
M5	7.71	23.06
M6	7.16	16.65
M7	-	16.65
M11	10.55	16.54
M12	9.64	2.41
M13	11.5	12.94
M14	11.4	19.86
M15	11.11	22.92
M16	3.63	16.75
M17	5.08	16.7

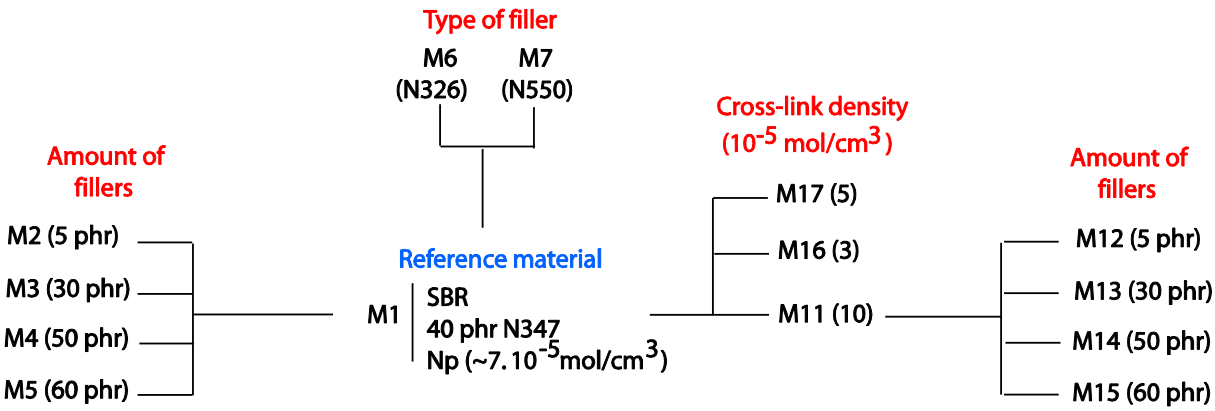

Figure 1 Material strategy and notations

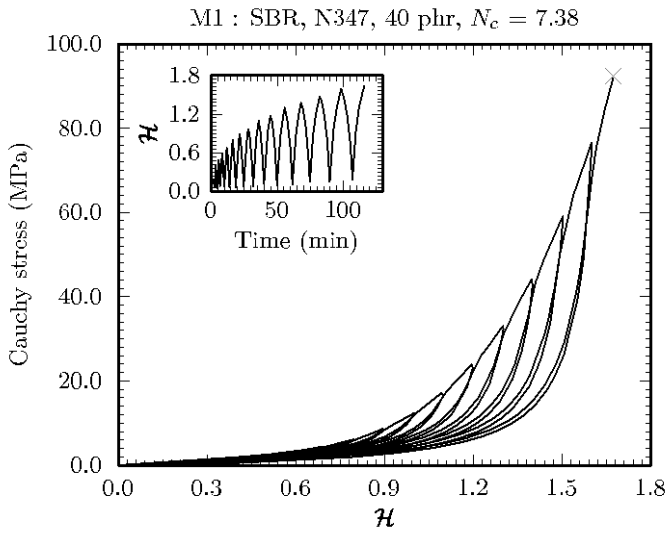

Figure 2 Material M1 stress-strain response to a uniaxial tensile cyclic test.

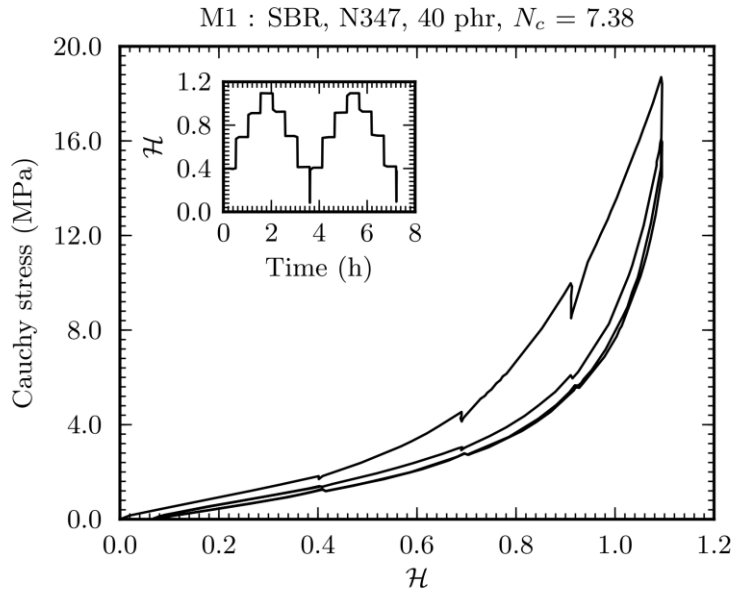

Figure 3 Material M1 stress-strain response to a two-cycle test, run at constant control strain rate of 10^{-2} s^{-1} with 30 minutes relaxation every 50% strain step.

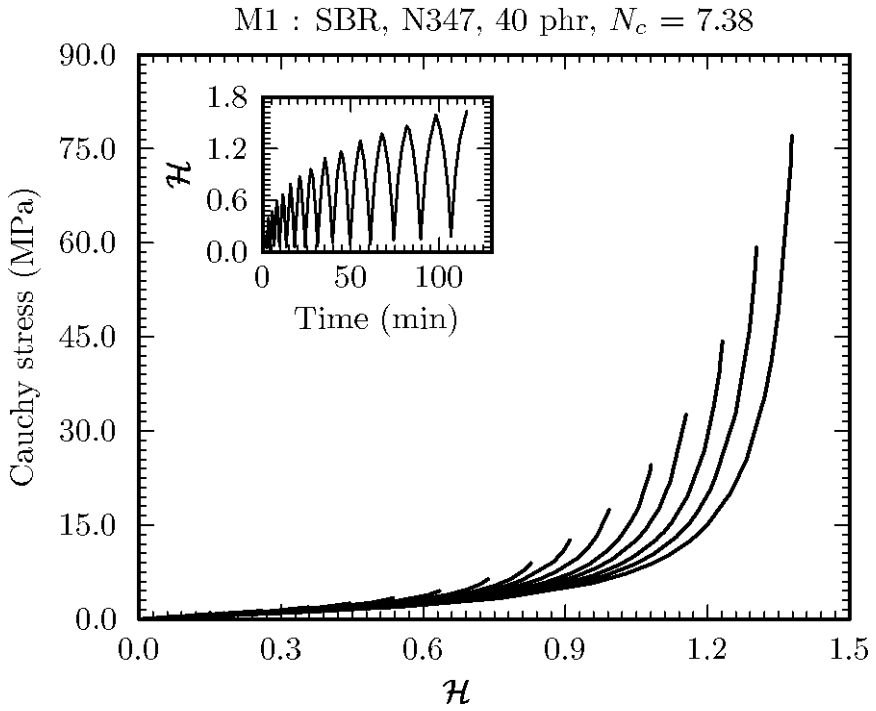

Figure 4. Stress-strain responses of material M1 softened by previous loadings to various strain levels.

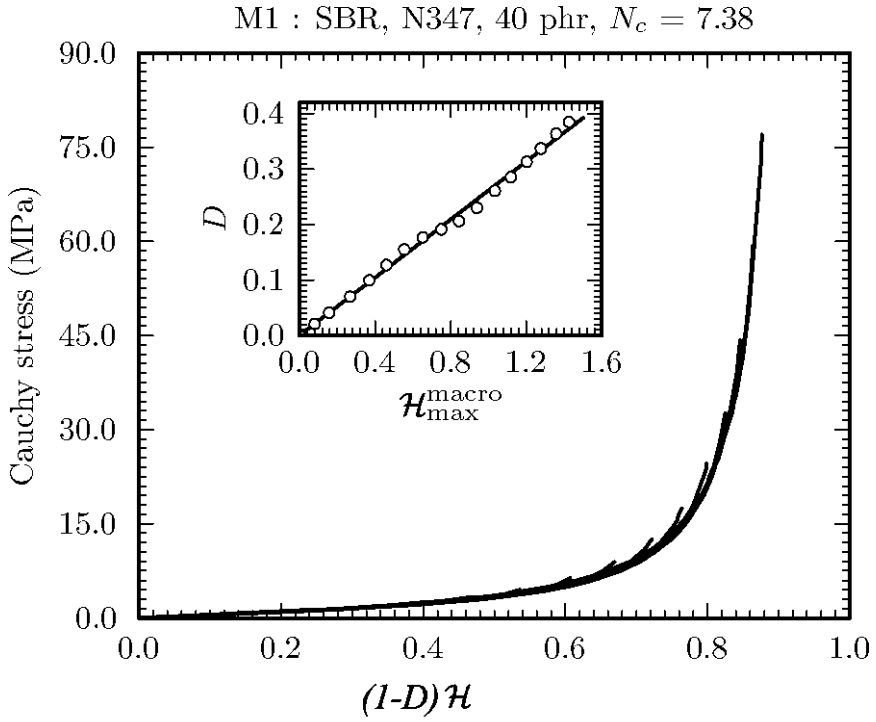

Figure 5 Material M1 master curver obtained by superposition of the stress-strain responses plotted in Fig. 3. In the inset graph, values of $D(H_{max})$ that provide a satisfying superposition

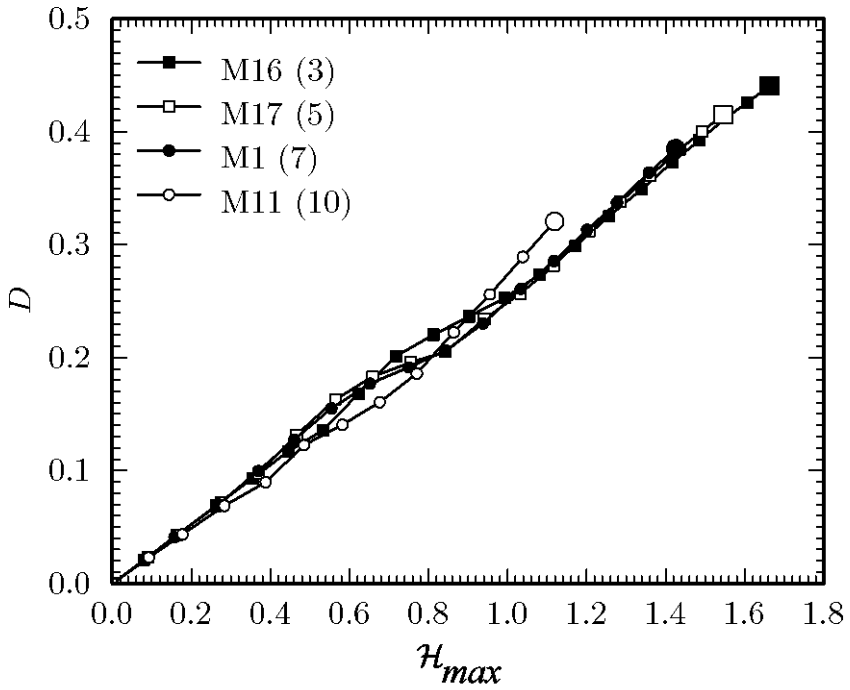

Figure 6 Evolution of the damage parameter with $D(H_{max})$ for materials with various cross-link densities N_c and a similar filler volume fraction $\varphi \sim 0.166$ (40 phr)

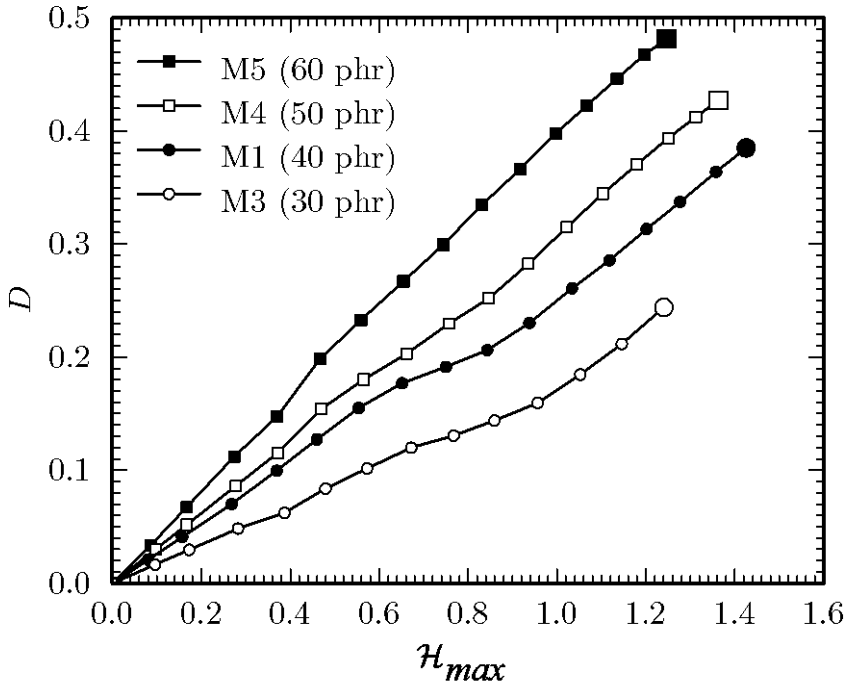

Figure 7 Evolution of the damage parameter with H_{max} for different amounts of carbon-black in materials with a similar cross-link density $N_c \sim 7.\ 10^{-5}$ mol/cm^3.

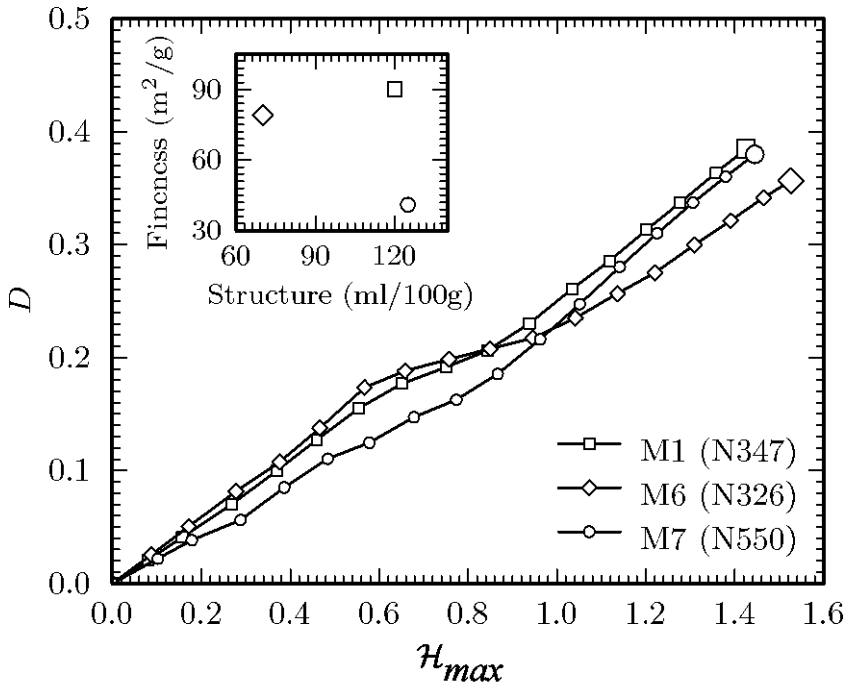

Figure 8 Effect of the type of carbon-black on the evolution of the damage parameter with H_{max} for materials with a similar amount of carbon-black (40 phr) and cross-link density $N_c \sim 7.\ 10^{-5}$ mol/cm^3.

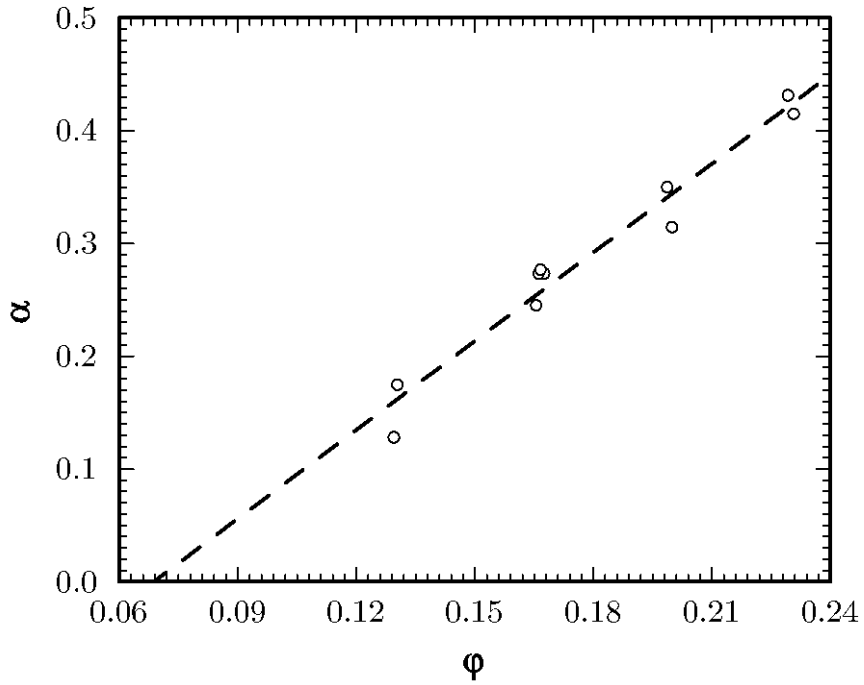

Figure 9 Evolution of the parameter α with the filler volume fraction φ for materials filled with a N347 carbon-black fillers.

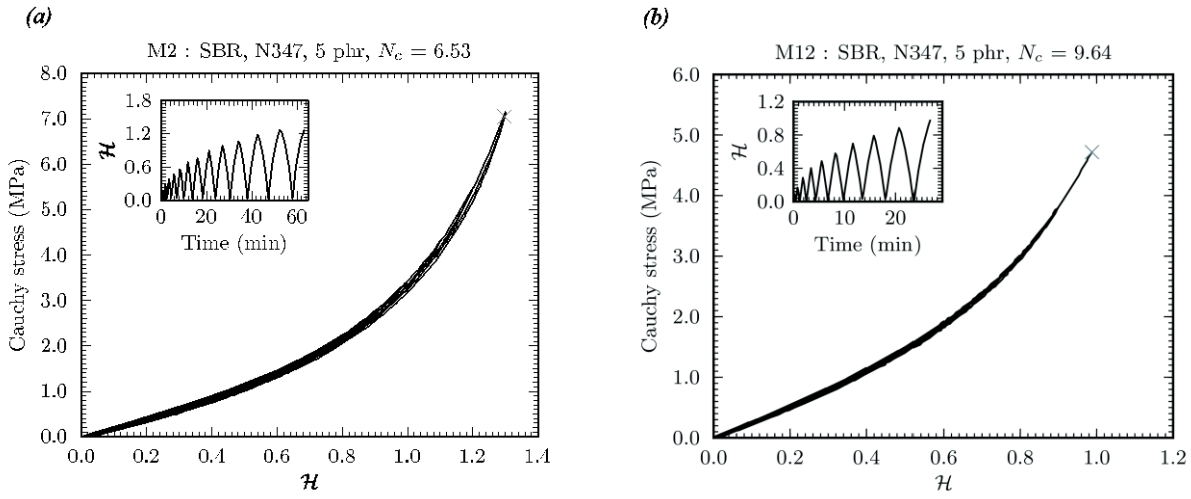

Figure 10 Stress-strain responses of materials M2 (a) and M12 (b) to a cyclic uniaxial tensile test.

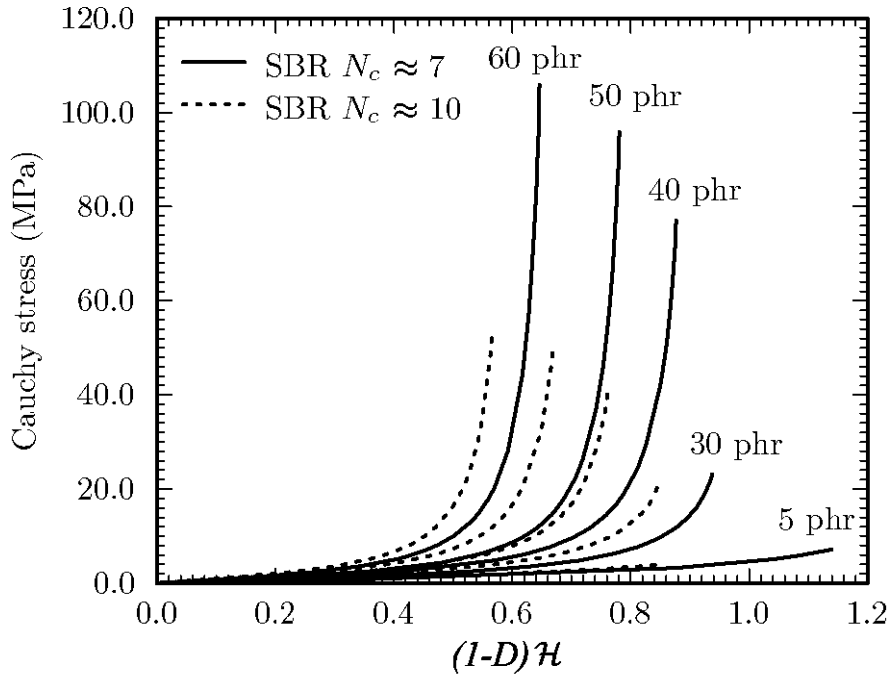

Figure 11 Uniaxial tension stress-strain responses of virtual virgin materials compared to material M1 to M5 with solid lines and M11 to M15 with dotted lines.

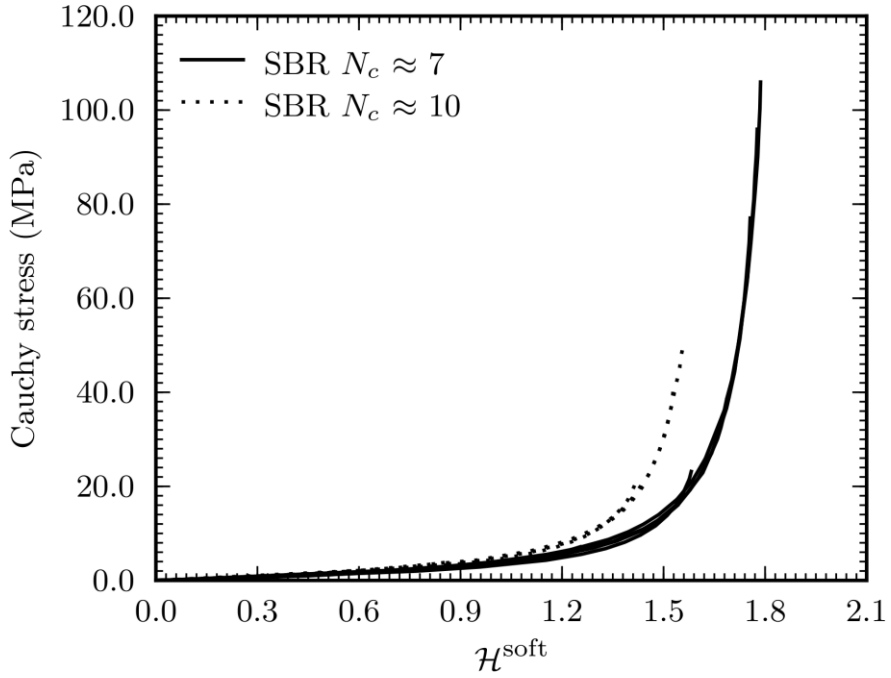

Figure 12 Superposition of the virgin material master curves onto the stress-strain behaviour of the soft domains by using the strain intensity factor *X* defined in (1).

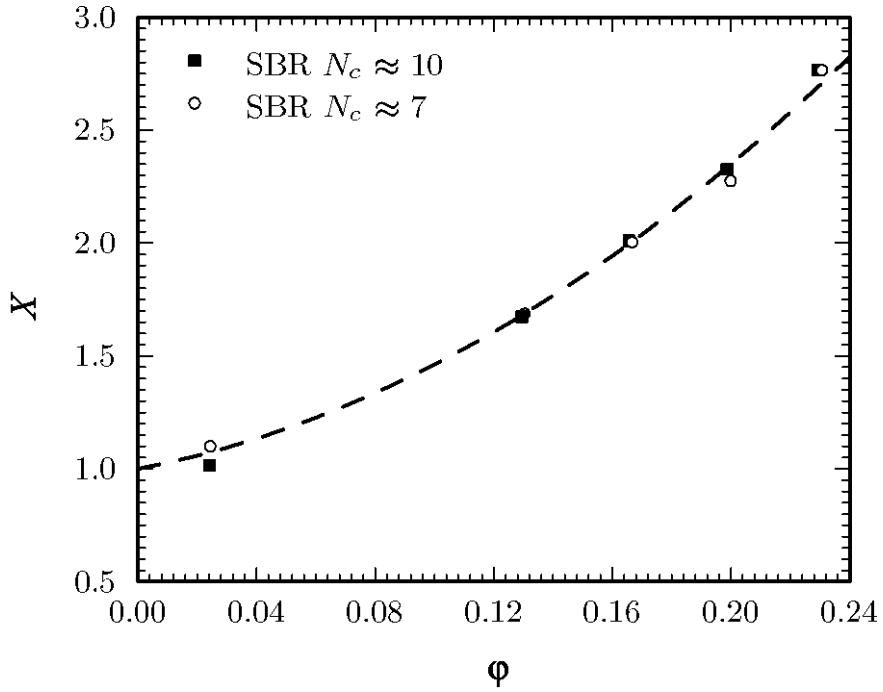

Figure 13 Evolution of parameter *X* with the filler volume fraction φ for two cross-link densities.